

## COMMUNICATION



# The icephobic performance of alkyl-grafted aluminum surfaces†

 S. A. Kulinich,<sup>\*ab</sup> M. Honda,<sup>a</sup> A. L. Zhu,<sup>c</sup> A. G. Rozhin<sup>b</sup> and X. W. Du<sup>d</sup>

 Cite this: *Soft Matter*, 2015, 11, 856

Received 4th October 2014

Accepted 5th December 2014

DOI: 10.1039/c4sm02204a

[www.rsc.org/softmatter](http://www.rsc.org/softmatter)

This work analyzes the anti-icing performance of flat aluminum surfaces coated with widely used alkyl-group based layers of octadecyltrimethoxysilane, fluorinated alkylsilane and stearic acid as they are subjected to repeated icing/deicing cycles. The wetting properties of the samples upon long-term immersion in water are also evaluated. The results demonstrate that smooth aluminum surfaces grafted with alkyl groups are prone to gradual degradation of their hydrophobic and icephobic properties, which is caused by interactions and reactions with both ice and liquid water. This implies that alkyl-group based monolayers on aluminum surfaces are not likely to be durable icephobic coatings unless their durability in contact with ice and/or water is significantly improved.

The formation of ice or wet-snow buildups on exposed surfaces may hinder the performance of aircraft, ships, power lines, wind turbines, offshore oil platforms and telecommunication systems.<sup>1–6</sup> Therefore, the prevention and control of ice accretion is of high potential in all these fields of human activity. The design and use of surfaces/coatings with minimum ice adherence and reduced ice accumulation is still actively considered as the most appealing and universal approach to the problem.<sup>3,5–20</sup> Most of the existing studies on anti-ice surfaces are focused on the reduction of ice adhesion strength<sup>1,5–8,10,19–24</sup> or delayed ice nucleation/formation.<sup>3,9,12,13,23,25,26</sup> Therefore lately the research in this area has been chiefly focused on the use and development of superhydrophobic surfaces (SHSs) for preventing ice formation and accumulation.<sup>4,9–11,13–23,25–29</sup> Significantly delayed ice formation<sup>3,10,12,13,15,16,23,26</sup> and reduced ice adhesion or

accumulation<sup>3,10,15–17,19,21,25</sup> have been reported for various SHSs. Theoretical models have also been developed, demonstrating how SHSs can delay ice formation from impinging water droplets,<sup>9,11,13</sup> which is in good agreement with experimental work.<sup>3,14,25,26</sup>

At the same time, several recent reports have raised doubts about SHSs as universal and durable anti-ice materials with long-term service and high efficiency under different conditions.<sup>1,13–16,22,27,29–31</sup> Relatively poor or reduced performance was reported for several types of SHSs tested under repeated icing/deicing conditions,<sup>15,16,22,29,31</sup> which was attributed to their poor abrasive resistance (also reported by others in a concise review<sup>32</sup>). In parallel, SHSs were reported to lose their anti-icing performance in a humid atmosphere, when icing follows (or occurs simultaneously with) water condensation or frost formation in their rough structures.<sup>2,13,16,22,33</sup> It is now therefore clear that SHSs may only be efficient anti-icing materials under low humidity conditions,<sup>9,13,16,22,33</sup> while their use as a universal remedy for ice accretion, *i.e.* under a very wide range of atmospheric conditions, may be very limited.<sup>1,2,13,16,22,33</sup> In a similar way, a recent study reported by Rykaczewski and co-authors<sup>34</sup> also raised doubts about the universal use of another class of rough anti-icing materials, *i.e.* so-called lubricant-impregnated surfaces (having rough surfaces infused with water-immiscible liquid).

Furthermore, Jung and co-workers investigated the water freezing delay of supercooled microdroplets on untreated and coated surfaces ranging from hydrophilic to superhydrophobic and used the delay values to evaluate the materials' ice-phobicity.<sup>14</sup> Certain surfaces with nanometer-scale roughness and higher wettability were found to display unexpectedly long freezing delays, at least one order of magnitude longer than typical SHSs with larger hierarchical roughness and low wettability.<sup>14</sup> In light of the above results, it is now clear that SHSs may not necessarily offer the best choice as universal and highly efficient materials for anti-icing applications.<sup>1,2,13–16,22,29,33</sup> This implies that, amongst others, smooth surfaces should also be

<sup>a</sup>Institute of Innovative Science and Technology, Tokai University, Hiratsuka, Kanagawa 259-1292, Japan. E-mail: s\_kulinich@yahoo.com

<sup>b</sup>School of Engineering and Applied Science, Aston University, Birmingham B4 7ET, UK

<sup>c</sup>Department of Chemical and Biological Engineering, University of British Columbia, Vancouver, BC, Canada V6T 1Z4

<sup>d</sup>School of Materials Science and Engineering, Tianjin University, Tianjin 300072, China

† Electronic supplementary information (ESI) available. See DOI: 10.1039/c4sm02204a

studied as alternative and (importantly) mechanically more stable candidates.<sup>5,14,16,22</sup>

In this communication, we report on the long-term anti-icing performance of several alkyl-terminated surfaces prepared on the surface of aluminum *via* conventional wet-chemistry methods widely used in the literature.<sup>35–37</sup> Smooth alkyl-grafted surfaces were previously proposed as ice-repellent materials<sup>5,8</sup> and the adhesion strength of ice on such surfaces was demonstrated to be reduced by a factor of  $\sim 3$  compared to mirror-polished aluminum.<sup>5</sup> However, no systematic evaluation of such materials over numerous icing/deicing cycles has been performed up to date. Through a series of subsequent icing/deicing tests repeated on several samples grafted with different alkyl groups, we demonstrate that such thin layers slowly react with ice (or cold water), which leads to their slow deterioration. In order to improve the surface density of alkyl-groups (which, hypothetically, might enhance the durability of such layers), we then used several strategies previously reported in the literature and prepared three different underlayers with a presumably higher density of surface hydroxyl groups,<sup>38–40</sup> which were then coated with a fluoro-alkyl layer. The anti-icing performance of the latter two-layer samples was also tested over icing/deicing, however no significant improvement in the long-term durability was achieved.

All samples tested in this work were prepared on aluminum alloy substrates (AA2024,  $55 \times 35 \times 2.0$  mm<sup>3</sup> in size). The Al substrates were initially mirror-polished (subsequently with 1.0 and 0.5  $\mu\text{m}$  sized alumina) and sonicated in water for 5 min, after which they were ultrasonically cleaned in methanol and ethanol (10 min each). Then the substrates were dried in air for 1 h, which allowed formation of a thin oxide layer, prior to further immersion into coating baths. The chemical baths used for coating contained 1.0% of octadecyltrimethoxysilane (ODTMS, from Fisher Scientific),<sup>35</sup> 1.0% of heptadecafluorodecyl-trimethoxysilane (FAS, from Shin Etsu Chemical Co.),<sup>36</sup> or 5.0 mM stearic acid (SA, from Wako).<sup>37</sup> The solvents were ethanol/water (9 : 1 v/v),<sup>35</sup> methanol/water (9 : 1 v/v),<sup>36</sup> and pure ethanol,<sup>37</sup> respectively. All the coating protocols applied in this study are widely used by others and their description can be found in greater detail elsewhere.<sup>35–37</sup> The modified surfaces were removed from the baths, rinsed with corresponding solvents, ethanol or methanol, and finally blow-dried with N<sub>2</sub> and oven-dried in air at 120 °C for 2 h and then at 50 °C for 10 h. Each sample was prepared as six duplicates to test the reproducibility of its properties and anti-icing performance. The results shown below thus present average values measured for six samples each.

Two-layer coatings were prepared in an attempt to increase the surface density of hydroxyl groups (and thus enhance the surface density of subsequently grafted fluoro-alkyl groups).<sup>38</sup> Three (smooth) underlayers with different chemistries were first prepared and then coated with a FAS monolayer following the same protocol as described above for the FAS single layer samples. Tetraethoxysilane (TEOS) was used to prepare a hydrated silica-based underlayer, following the protocol previously developed by Meth and Sukenik to increase the surface OH group density.<sup>38</sup> Mirror-polished Al samples were sonicated

in methanol, after which a hydrated SiO<sub>2</sub> layer (with a high density of surface hydroxyl groups<sup>38</sup>) was prepared by successive immersion in neat TEOS ( $\sim 15$  s) followed by immersion in deionized (DI) water for 2 min, followed by drying with a N<sub>2</sub> gas flow. Immersion in both TEOS and water was repeated 5 times, after which the samples were kept in water for at least 1 h and then rinsed well with DI water. Finally, the samples were blown with nitrogen and immersed in a FAS bath for grafting with fluoroalkyl groups.<sup>38</sup> For convenience, the samples are hereafter denoted as TEOS/FAS.

The second series of samples were first coated with a bis-1,2-(triethoxysilyl)ethane (BTSE, from Sigma-Aldrich) layer, following the method previously reported by Franquet and co-authors.<sup>39</sup> In order to provide a maximum amount of silanol groups (and consequently, the highest surface density of hydroxyl groups), the pH was kept in the range of 4.5–5.0.<sup>39</sup> A 4.0% BTSE bath (v/v) was used, with the dip-coating time set as 100 s, to provide an underlayer thickness on the order of 100 nm,<sup>39</sup> and the samples were finally dried in air prior to further treatment with FAS. This series is further denoted as BTSE/FAS.

The third group of samples were first coated with a permanganate conversion coating (PCC), which is based on hydrated MnO<sub>2</sub> and thus was also expected to provide a large surface density of OH groups. The polished and cleaned samples were immersed in a KMnO<sub>4</sub>-borax bath at 68 °C following the coating method described in greater detail elsewhere.<sup>40,41</sup> After 3 min they were removed, rinsed with DI water, blown with N<sub>2</sub> and then grafted with FAS. Hereafter, the samples are referred to as PCC/FAS.

The wetting properties of the samples (water contact angle, CA, and contact angle hysteresis, CAH) were assessed on a commercial contact-angle goniometer (CAX, Kyowa Interface Science) following standard procedures. CA (and CAH) values were measured by the sessile-drop method: small water droplets (5  $\mu\text{L}$  in volume) were gently placed on the surface, and their shape was evaluated by using the goniometer optics and software. The CA values reported here were the averages of at least five measurements on various parts of each sample. Scanning electron microscopy (SEM, JSM 6330 from JEOL) was used to take surface images of the samples. X-ray photoelectron spectroscopy (XPS) analysis was performed using a Leybold MAX200 spectrometer.

The adhesion of ice was evaluated (as the shear stress of ice detachment) using a custom-built centrifuge-type apparatus similar to those described elsewhere.<sup>10,16,19,29</sup> The tested ice was of glaze type and prepared by spraying super-cooled microdroplets of water in a wind tunnel at a subzero temperature of  $-10$  °C (thus simulating “freezing rain” conditions). The ice preparation procedure was also previously described in more detail elsewhere.<sup>10,16,19,29</sup> Samples, iced in a wind tunnel, were then spun in a centrifuge at a constantly increasing speed. The shear stress was calculated by taking into account the mass and area of detached ice and by precisely detecting the rotational speed of the sample at the moment of (adhesive) ice failure. The procedure was previously described in more detail elsewhere.<sup>10,16,19,29</sup> Uncoated mirror-polished aluminum was used as a standard reference sample, demonstrating the shear stress of

ice detachment on its surface of  $359 \pm 35$  kPa and agreeing with values previously reported in the literature.<sup>10,16,19</sup>

Fig. 1a and b present surface images of a smooth FAS-coated sample which was kept in air for about twelve months. The as-prepared sample demonstrated similar surface features, implying that the FAS-coated sample was protected well and did not demonstrate any signs of corrosion in air. The intermetallic particles (Al–Cu–Fe–Mn type in Fig. 1a and Al–Cu–Mg type in Fig. 1b) are seen to have smooth boundaries with the surrounding Al matrix. Such intermetallic particles (also known as second-phase particles) are known to form during alloy solidification and to be predominant chemical types on the surface of AA2024, making 12.3 (the irregular-shaped Al–Cu–Fe–Mn type) and 61.3 number % (the regular-shaped Al–Cu–Mg type) of all particles on its surface.<sup>40,41</sup> No signs of corrosion are observed around the second-phase particles as shown in Fig. 1a and b and their boundaries reveal no trenches or corrosion products.

For comparison, Fig. 1c–e demonstrate surface images of the same FAS-coated sample after thirty-three subsequent icing/deicing events. While the surface of the Al matrix was found to be mainly unchanged, trenches are now observed around many intermetallic particles as shown in Fig. 1c–e. Such trenches are well-known to result from electrochemical corrosion processes occurring in the presence of aqueous electrolytes contacting the AA2024 surface with insufficient protection.<sup>41</sup> Very similar results were also observed for SA- and ODTMS-treated AA2024 samples. Similar to the sample coated with FAS (Fig. 1), the as-prepared SA- and ODTMS-coated samples also demonstrated no sign of surface corrosion, while clear pits and trenches were observed on their surfaces after 33–34 icing/deicing cycles (Fig. S1 and S2 in the ESI<sup>†</sup>). Therefore, it can be concluded that during numerous icing/deicing cycles, the alkyl-chain based layers deteriorated, and electrochemical corrosion processes started and gradually proceeded on the partially uncoated surfaces.

Fig. 2 presents how the shear stress of ice detachment changed as a function of the number of icing/deicing events on the FAS (a), SA (b) and ODTMS (c) coated AA2024 samples. It is clearly seen that the ice adhesion strength on all the three samples gradually increased over repeated icing/deicing tests. More specifically, while the shear stress of ice detachment values on the as-prepared samples was  $86.2 \pm 29$ ,  $98.1 \pm 43$  and  $87.5 \pm 34$  kPa (for the FAS, SA and ODTMS-coated surfaces, respectively), after as many as 33–34 icing/deicing tests, the values gradually increased and were in the range of  $\sim 150$  to  $\sim 175$  kPa, which implies a nearly two-fold increase in ice adhesion strength. Here, it should be noted that the shear stress of ice detachment values previously measured on several SHSs (with different surface chemistries and topographies) was initially lower on the as-prepared samples than those observed in Fig. 2a–c, but after about 22 icing/deicing cycles they were found to be  $\sim 175$  to  $\sim 200$  kPa.<sup>16</sup> Since both the sample geometries and techniques used in the present study and work<sup>16</sup> were similar, this finding is probably explained by the gradually increased ice/solid contact area as the rough structures of the SHSs were gradually damaged during icing/deicing, eventually leading to smoother and less spiky surfaces after as many as 22 icing/deicing cycles.<sup>16</sup> Meanwhile, the mechanisms involved in the degrading ice repellency of flat surfaces presented in Fig. 2 are different as they are not related to any mechanical breakage of rough surface asperities and change in the ice/solid interface area.

The results presented in Fig. 1 and 2 allowed us to hypothesize that all the alkyl mono-layers prepared in this study, being efficient enough to protect the AA2024 samples in air, were not dense enough to prevent water molecules from penetrating through the layers and reaching the alkyl chain–alloy interface. The bonds between the organosilane molecules and the metal surface are known to form through the condensation reaction, in which the silanol group (–Si–OH) combines

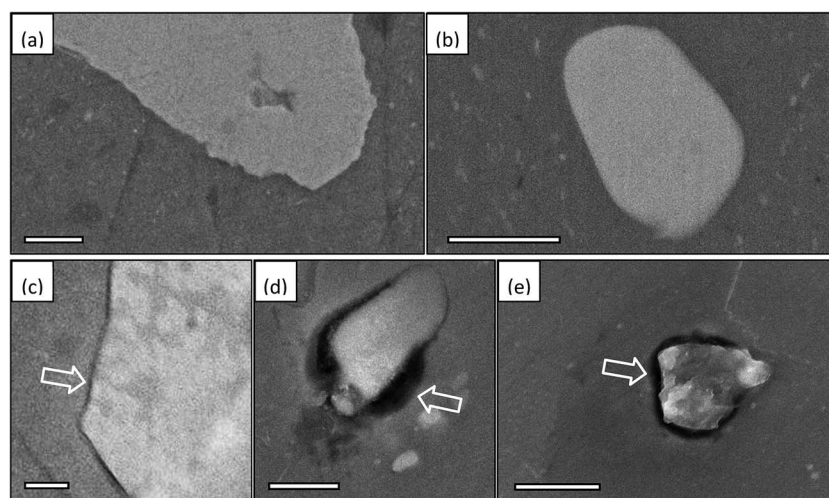


Fig. 1 SEM surface images of polished AA2024 sample coated with FAS: (a and b) after twelve months in air and (c–e) after 33 icing/deicing events. Irregular (a and c) and regular (b, d and e) intermetallic particles and their vicinities are shown. Scale-bars indicate  $1 \mu\text{m}$ . Trenches electrochemically formed between the particles and the surrounding Al matrix are indicated by arrows.

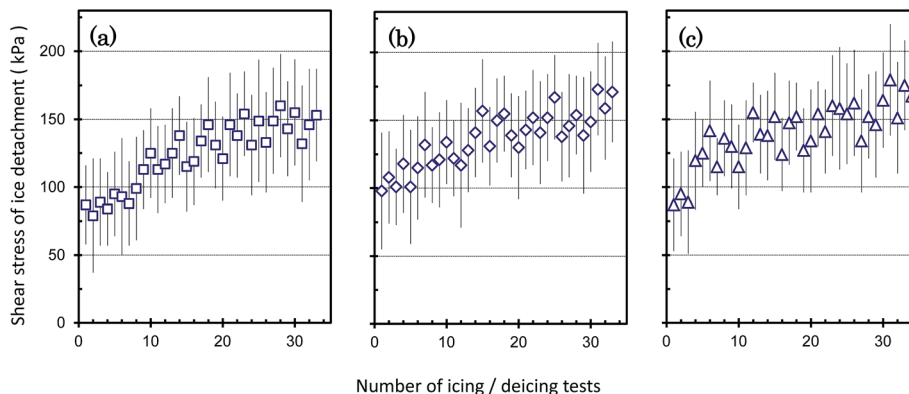
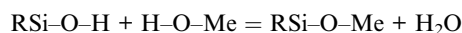


Fig. 2 Shear stress of ice detachment as a function of icing/deicing cycles on (a) FAS, (b) SA and (c) ODTMS-treated surfaces.

with the surface metal hydroxyl group (Me–OH), releasing water and forming the metallo-siloxane bond Me–O–Si:<sup>5,36,39,42</sup>



However, the above reaction is reversible,<sup>42</sup> though no experimental results are easily available in the literature to support this fact. This implies that, in principle, the Me–O–Si bond may be hydrolyzed, given that water molecules and time are available.<sup>42</sup> Thus, the RSi–O–Me bonds may be hydrolyzed back to silanol groups, resulting in surface metal hydroxyl groups Me–OH and loose alkylsilanol molecules RSi–O–H.<sup>42</sup> This is what we believe happened gradually when the alkyl-grafted Al samples were subjected to repeated icing/deicing cycles. Based on the results presented in Fig. 1 and 2, we postulate that the prepared alkyl-based layers were not dense enough to protect the RSi–O–Me bonds from water molecules. The latter molecules were believed to penetrate slowly towards such bonds and hydrolyze them, which led to a partial detachment of organic molecules and exposure of the uncoated substrate. On the other hand, the contact of the uncoated AA2024 surface with water is well-known to result in gradual electrochemical corrosion processes, which are expected primarily at the intermetallic–Al matrix interface.<sup>41</sup> The results of such electrochemical corrosion processes are indeed observed in Fig. 1c–e, which supports the above assumption. As a result, the formed corrosion products, along with the partially exposed alloy surface (both of which are typically hydrophilic metal oxides and hydroxides), were expected to lead to the gradually increased ice adhesion strength observed in Fig. 2.

In an attempt to increase the surface density of alkyl chains, we therefore prepared three two-layer samples with different underlayers which were previously reported to have a high surface density of OH groups.<sup>38–40</sup> Such underlayers, upon further coating with a FAS layer, were expected to provide higher densities of surface alkyl groups (see experiment description above and Fig. S3 in the ESI†). However, no significant improvement was found in the icephobic performance of the three two-layer surfaces over repeated icing/deicing, as they also demonstrated trends similar to those presented in Fig. 2 for

one-layer alkyl-grafted counterparts (see Fig. S4 in the ESI†). This probably implies that similar surface deterioration mechanisms were also involved when the two-layer samples contacted with ice and/or water. On the other hand, it is also possible that the three underlayers with different chemistries used in this study (based on hydrated silica,<sup>38</sup> BTSE<sup>39</sup> and hydrated MnO<sub>2</sub> (ref. 40 and 41)) did not provide significantly larger surface densities of OH groups, which in turn did not result in any noticeable improvement in the alkyl-group surface density compared to the AA2024 sample directly coated with FAS as one layer.

The SEM surface images of the two-layer samples did not differ noticeably after repeated icing/deicing tests (Fig. S3†), which is different from the results presented in Fig. 1 for one-layer samples. This can be easily explained by the presence of underlayers on their surface, which were at least 100 nm thick and thus could act as a good physical barrier that efficiently protected the underlying metal surface from corrosion even when the topmost FAS layer partially degraded. The decay of the topmost layer, however, was believed to follow the same mechanisms when the two-layer samples contacted ice and cold water, since their ice-repellent performance trends over icing/deicing were qualitatively similar to those of their one-layer alkyl-grafted counterpart (see Fig. 2 and S4†).

To lend support to the above hypothesis on the deterioration of alkyl-based layers in contact with ice, the icing/deicing tests were accompanied by CA measurements. Fig. 3a and b show how water CA values evolved on the surface of the one-layer FAS (a) and SA (b) coated samples as a function of the number of icing/deicing events (the trend on the ODTMS-coated sample was very similar and is shown in Fig. S5†). The wetting hysteresis (CAH) of the same samples was also evaluated and the results are presented in Fig. S6.† In agreement with the trends presented in Fig. 2a and b, the samples are seen in Fig. 3a and b, S5 and S6† to lose their hydrophobicity as their water CA values steadily decrease and CAH values gradually increase when the samples are repeatedly iced and then mechanically deiced.

For comparison, Fig. 3c shows how the FAS (open circles) and SA (solid circles) coated AA2024 samples changed their CA values over time upon immersion in DI water at room

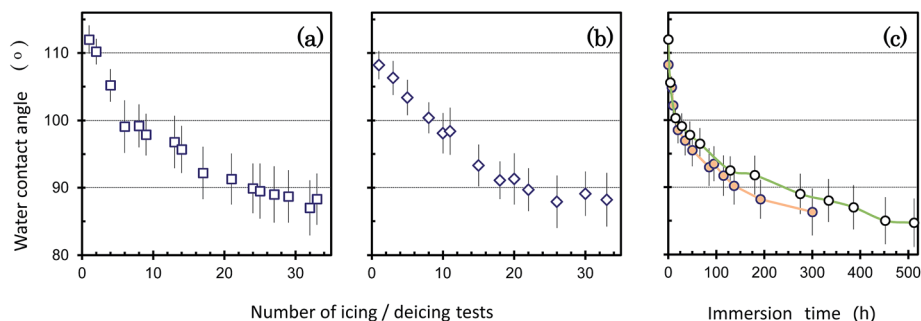


Fig. 3 Evolution of water CA values for (a) FAS and (b) SA coated samples over icing/deicing tests. (c) CA values for FAS (open symbols) and SA (solid symbols) coated samples as a function of immersion time (in DI water). Lines are only given as a guide to the eye.

temperature. It is clearly seen that the samples gradually lose their hydrophobic properties in contact with water, as their CA values gradually decrease to  $\sim 85^\circ$  after immersion for  $\sim 300$  to 500 h. This observation is consistent with both the results presented in Fig. 3a and b and the above discussion. Note that the samples presented in Fig. 3a and b demonstrated water CA values of  $\sim 90^\circ$  after  $\sim 30$  icing events, which implied an accumulative contact with cold water for at most  $\sim 15$ – $20$  h (if the contact with ice is not taken into consideration). The curves in Fig. 3c exhibit that similar values of CA were observed when the same samples were immersed in DI water for as long as  $\sim 200$  h. The difference may be explained by the use of tap water in the icing experiments and DI water in the immersion experiments. Since corrosion related processes are accelerated in the presence of ions/electrolytes, this may explain well why the hydrophobicity of the FAS- and SA-coated samples degraded faster during icing/deicing (Fig. 3a and b) compared to similar samples simply immersed in DI water (Fig. 3c).

The above explanations are also supported by XPS results (see Table S1 in the ESI†) which were obtained for the ODTMS-coated sample both before and after icing/deicing treatment. The amount of Si atoms (*i.e.* mainly those belonging to ODTMS molecules) in the topmost surface layer of the sample was reduced by  $\sim 30\%$  after the sample was iced/deiced thirty-four times. This agrees well with the above proposed gradual loss of ODTMS molecules as a result of partial hydrolysis in contact with water and ice followed by their further removal during ice detachment.

It should be mentioned that the long-term stability of alkylsilane, fluoroalkylsilane or fatty acid based coatings in contact with water has not been well-studied, the number of such reports being very scarce and normally limited to the Si or GaN surface as a substrate.<sup>43,44</sup> The Si surface coated with a long-chain aliphatic self-assembled monolayer of octadecyltrichlorosilane was reported to exhibit no considerable changes in its CA after as long as 24 h of exposure to water.<sup>43</sup> At the same time, a GaN surface coated with octadecyltrichlorosilane (which was attached to a thin  $\text{Ga}_2\text{O}_3$  toplayer) was recently shown to lose its hydrophobic properties in contact with aqueous media.<sup>44</sup> A recent study by Boinovich and Emelyanenko has reported on a gradual deterioration of various organosilane layers covering superhydrophobic surfaces.<sup>45</sup> Considering their

findings, it is now possible to assume that both water and ice repellencies of some SHSs reported in studies<sup>16,22,29</sup> deteriorated not only because of their rough structures being mechanically abraded during icing/deicing but also owing to the chemical reactions between surface-grafted organosilane or fatty acid molecules with water and/or ice.

As a final remark, it is worth noting that a large number of icephobic surfaces proposed and developed thus far, especially many of those based on SHSs, are often passivated with alkyl or fluoroalkyl surface groups.<sup>5,12,15,16,22,25,29,46,47</sup> Since the present work raises doubts about the durability of alkyl-grafted aluminum surfaces, it now looks reasonable that many (if not all) organosilane- or fatty acid-coated surfaces may be not durable enough when they are subjected to numerous icing and deicing events. While, ideally, icephobic coatings for outdoor applications should survive for years or even decades without any significant deterioration, the alkyl-coated surfaces may not meet this requirement as they appear to lose their water- and ice-repellent properties much faster. In light of this, potential icephobic coatings based on other materials (*e.g.*, polymers, silicones, *etc.*) may also need more careful evaluation, as their long-term performance in contact with water and ice may turn out not to be satisfactory, too.

In summary, this work reports on how the anti-icing properties of smooth alkyl- and fluoroalkyl-grafted aluminum surfaces are influenced by repeated icing/deicing cycles. It is demonstrated experimentally that surfaces coated with fluoroalkylsilane, alkylsilane and stearic acid gradually deteriorate and lose their ice repellency when subjected to numerous icing/deicing events. Similarly, two-layer coatings, with hydrated silica, hydrated  $\text{MnO}_2$  or bis-1,2-(triethoxysilyl)ethane underlayers (all the three used to provide presumably higher densities of surface alkyl groups), also exhibited gradually increasing ice adhesion strength when tested under the same conditions. In parallel, the water-repellent properties of all the samples were also found to deteriorate gradually. The results suggest that the applied organic molecules could not provide dense enough surface layers, which allowed water molecules to reach the alkyl layer/substrate interface and make the organic layer deteriorate gradually. The findings also imply that the chemical stability of all potential anti-ice materials in contact with water and ice should be carefully addressed and evaluated in the future.

## Acknowledgements

The help from Dr K. Nose (of UACJ Corp., Nagoya, Japan) with surface analysis of samples is greatly acknowledged. S.A.K. also acknowledges the Marie Curie International Incoming Fellowship from the European Commission.

## References

- 1 M. Susoff, K. Siegmann, C. Pfaffenroth and M. Hirayama, *Appl. Surf. Sci.*, 2013, **282**, 870–879.
- 2 R. Karmouch and G. G. Ross, *Appl. Surf. Sci.*, 2010, **257**, 665–669.
- 3 R. Ramachandran and M. Nosonovsky, *Soft Matter*, 2014, **10**, 7797–7803.
- 4 S. A. Kulinich and M. Farzaneh, *Appl. Surf. Sci.*, 2004, **230**, 232–240.
- 5 B. Somlo and V. Gupta, *Mech. Mater.*, 2001, **33**, 471–480.
- 6 V. K. Croutch and R. A. Hartley, *J. Coat. Technol.*, 1992, **64**, 41–52.
- 7 T. Bharathidasan, S. V. Kumar, M. S. Bobji, R. P. S. Chakradhar and B. J. Basu, *Appl. Surf. Sci.*, 2014, **314**, 241–250.
- 8 V. F. Petrenko and S. Peng, *Can. J. Phys.*, 2003, **81**, 387–393.
- 9 A. Alizadeh, M. Yamada, R. Li, W. Shang, S. Otta, S. Zhong, L. Ge, A. Dhinojwala, K. R. Conway, V. Bahadur, A. J. Vinciguerra, B. Stephens and M. L. Blohm, *Langmuir*, 2012, **28**, 3180–3186.
- 10 S. A. Kulinich and M. Farzaneh, *Langmuir*, 2009, **25**, 8854–8856.
- 11 V. Bahadur, L. Mishchenko, B. Hatton, J. A. Taylor, J. Aizenberg and T. Krupenkin, *Langmuir*, 2011, **27**, 14143–14150.
- 12 L. Boinovich, A. M. Emelyanenko, V. V. Korolev and A. S. Pashinin, *Langmuir*, 2014, **30**, 1659–1668.
- 13 L. Oberli, D. Caruso, C. Hall, M. Fabretto, P. J. Murphy and D. Evans, *Adv. Colloid Interface Surf.*, 2014, **210**, 47–57.
- 14 S. Jung, M. Dorrestijn, D. Raps, A. Das, C. M. Megaridis and D. Poulikakos, *Langmuir*, 2011, **27**, 3059–3066.
- 15 Y. N. Wang, J. Xue, Q. J. Wang, Q. M. Chen and J. F. Ding, *ACS Appl. Mater. Interfaces*, 2013, **5**, 3370–3381.
- 16 S. A. Kulinich, S. Farhadi, K. Nose and X. W. Du, *Langmuir*, 2011, **27**, 25–29.
- 17 L. B. Boinovich, A. M. Emelyanenko, V. K. Ivanov and A. S. Pashinin, *ACS Appl. Mater. Interfaces*, 2013, **5**, 2549–2554.
- 18 R. M. Fillion, A. R. Riahi and A. Edrissy, *Renewable Sustainable Energy Rev.*, 2014, **32**, 797–809.
- 19 S. A. Kulinich and M. Farzaneh, *Appl. Surf. Sci.*, 2009, **255**, 8153–8157.
- 20 Y. He, C. G. Jiang, X. B. Cao, J. Che, W. Tian and W. Z. Yuan, *Appl. Surf. Sci.*, 2014, **305**, 589–595.
- 21 H. Saito, K. Takai and G. Yamauchi, *Surf. Coat. Int.*, 1997, **80**, 168–171.
- 22 S. Farhadi, M. Farzaneh and S. A. Kulinich, *Appl. Surf. Sci.*, 2011, **257**, 6264–6269.
- 23 F. Arianpour, M. Farzaneh and S. A. Kulinich, *Appl. Surf. Sci.*, 2013, **265**, 546–552.
- 24 H. Murase, K. Nanishi, H. Kogure, T. Fujibayashi, K. Tamura and N. Haruta, *J. Appl. Polym. Sci.*, 1994, **54**, 2051–2062.
- 25 F. C. Wang, F. C. Lv, Y. P. Liu, C. R. Li and Y. Z. Lv, *J. Adhes. Sci. Technol.*, 2013, **27**, 58–67.
- 26 L. Q. Zheng, Z. R. Li, S. Bourdo, K. R. Khedir, M. P. Asar, C. C. Ryerson and A. S. Biris, *Langmuir*, 2011, **27**, 9936–9943.
- 27 M. Nosonovsky and V. Hejazi, *ACS Nano*, 2012, **6**, 8488–8491.
- 28 Z. W. Wang, Q. Li, Z. X. She, F. N. Chen, L. Q. Li, X. X. Zhang and P. Zhang, *Appl. Surf. Sci.*, 2013, **271**, 182–192.
- 29 S. A. Kulinich and M. Farzaneh, *Cold Reg. Sci. Technol.*, 2011, **65**, 60–64.
- 30 J. Che, J. Liu, M. He, K. Y. Li, D. P. Cui, Q. L. Zhang, X. P. Zeng, Y. F. Zhang, J. J. Wang and Y. L. Song, *Appl. Phys. Lett.*, 2012, **101**, 111603.
- 31 A. Lazauskas, A. Guobiene, I. Prosyčevs, V. Baltrušaitis, V. Grigaliūnas, P. Narmontas and J. Baltrusaitis, *Mater. Charact.*, 2013, **82**, 9–16.
- 32 T. Verho, C. Bower, P. Andrew, S. Franssila, O. Ikkala and R. H. A. Ras, *Adv. Mater.*, 2011, **23**, 673–678.
- 33 R. Karmouch and G. C. Ross, *J. Phys. Chem. C*, 2010, **114**, 4063–4066.
- 34 K. Rykaczewski, S. Anand, S. B. Subramanyam and K. K. Varanasi, *Langmuir*, 2013, **29**, 5230–5238.
- 35 L. Thomsen, B. Watts, D. V. Cotton, J. S. Quinton and P. C. Dastoor, *Surf. Interface Anal.*, 2005, **37**, 472–477.
- 36 X. Yao, Q. W. Chen, L. Xu, Q. K. Li, Y. L. Song, X. F. Gao, D. Quéré and L. Jiang, *Adv. Funct. Mater.*, 2010, **20**, 656–662.
- 37 W. R. Thompson and J. E. Pemberton, *Langmuir*, 1995, **11**, 1720–1725.
- 38 S. Meth and C. N. Sukenik, *Thin Solid Films*, 2003, **425**, 49–58.
- 39 A. Franquet, J. De Laet, T. Schram, H. Terryn, V. Subramanian, W. J. Van Ooij and J. Vereecken, *Thin Solid Films*, 2001, **384**, 37–45.
- 40 S. A. Kulinich, A. S. Akhtar, P. C. Wong, K. C. Wong and K. A. R. Mitchell, *Thin Solid Films*, 2007, **515**, 8386–8392.
- 41 S. A. Kulinich and A. S. Akhtar, *Rus. J. Non-Ferrous Met.*, 2012, **53**, 176–203.
- 42 W. J. van Ooij, *Tsinghua Sci. Technol.*, 2005, **10**, 639–664.
- 43 M. Maccarini, M. Himmelhaus, S. Stoycheva and M. Grunze, *Appl. Surf. Sci.*, 2005, **252**, 1941–1946.
- 44 C. Arisio, C. A. Cassou and M. Lieberman, *Langmuir*, 2013, **29**, 5145–5149.
- 45 L. Boinovich and A. Emelyanenko, *Adv. Colloid Interface Sci.*, 2012, **179–182**, 133–141.
- 46 F. Y. Lv and P. Zhang, *Appl. Surf. Sci.*, 2014, **321**, 166–172.
- 47 R. J. Liao, Z. P. Zuo, C. Guo, Y. Yuan and A. Y. Zhuang, *Appl. Surf. Sci.*, 2014, **317**, 701–709.